2

Material Analysis Using Characteristic Gamma Rays Induced by Neutrons

Alexander P. Barzilov, Ivan S. Novikov and Phillip C. Womble
Western Kentucky University
USA

1. Introduction

Neutron interrogation based methods of non-destructive analysis are well established techniques employed in the field of bulk material analysis. These methods utilize a source of neutrons (a neutron probe) to irradiate objects under scrutiny. Nuclear reactions initiated by neutrons in the volume of the irradiated sample include the following: inelastic neutron scattering, thermal neutron capture, and neutron activation. As a result of nuclear reactions with the material inside the object, the "fingerprint" γ-rays are emitted with characteristic energies. These characteristic gamma rays are used for the elemental identification. By measuring and counting the number of γ-rays emitted with a specific energy, one can deduce the amount of the associated chemical element in the sample. The amounts of chemical elements measured allow specifying the chemical composition of the analyzed sample.

Neutron technique is an excellent choice to rapidly determine elemental content of the sample *in situ* in non-intrusive manner. It is a great fit for in situ applications that involve samples that are hard to reach or unsafe to handle, and that require the analysis to be performed rapidly, in real time.

Accelerator based neutron sources such as deuterium – deuterium (d-d) and deuterium – tritium (d-t) fusion neutron generators provide the electronic control of neutron emission including its time structure. The pulse mode of neutron production allows the use of coincidence methods to segregate prompt and delayed gamma ray signatures emitted from neutron induced nuclear reactions. The kinematics of fusion reactions allows "tagging" of outgoing neutrons using the associated particles.

The pulse neutron systems are used in industry for analysis of coal (Dep et al., 1998; Sowerby, 2009), cement (Womble et al., 2005), metal alloys (James & Fuerst, 2000), in geological and soil analysis (Wielopolski et al., 2008), and oil well logging (Nikitin & Bliven, 2010). Security applications of neutron based systems are for chemical and explosive threats detection (Vourvopoulos & Womble, 2001; Aleksandrov et al., 2005; Lanza, 2006), including the search for threats in cargo containers (Barzilov & Womble, 2003) and vehicles (Reber et al., 2005; Koltick et al., 2007), humanitarian demining and confirmation of unexploded ordinance (Womble et al., 2002; Holslin et al., 2006). Such technologies are considered in astrochemistry applications for in situ analysis of planetary samples (Parsons et al., 2011).

The use of the pulse neutron based analysis of nitrogen and oxygen content *in vivo* is discussed in nutrition research (Shypailo & Ellis, 2005) and in cancer diagnostics (Maglich & Nalcioglu, 2010).

In the presented chapter we discuss the components of pulse neutron based material analysis systems, nuclear reactions induced by neutrons, characteristic gamma radiation emitted in these nuclear reactions, gamma ray spectral analysis methods for elemental characterization, and "neutrons in – photons out" methods that utilize the characteristic gamma radiation.

2. Pulse neutron sources and system components

A pulse neutron based material analysis system consists of a neutron source, gamma and particle radiation detector(s), a shadow radiation shielding to cover detectors from direct source neutrons, and associated hardware and software for system control, data acquisition and processing. Fig.1 shows the scheme of a typical system. The system operates as follows. Emitted by a source neutrons induce nuclear reactions in the irradiated object and excite nuclei. Excited nuclei emit photons due to various de-excitation processes that are measured by a gamma ray detector. The gamma ray spectrum is analyzed providing information on the chemical composition of the irradiated sample.
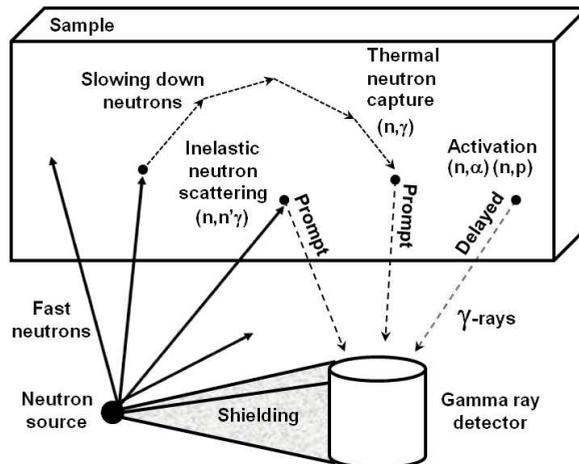

Fig. 1. Pulse neutron based elemental analysis scheme

Various radioisotopes, neutron beams from a nuclear reactor core, or accelerator-based devices are used as neutron sources. Radioisotopes used in neutron sources include ^{252}Cf, ^{239}Pu, ^{241}Am, and others. Californium-252 undergoes spontaneous fission with emission of neutrons with the average energy 2.5 MeV. The ^{252}Cf neutron emission spectral distribution is described by the semi-empirical Watt formula. Plutonium and americium based sources emit neutrons using alpha decay of ^{239}Pu or ^{241}Am and (α,n) reactions in the matrix of light elements such as beryllium or lithium. The neutron energy spectrum of these sources is wide (up to ~11 MeV) with the average neutron energy ~4.5 MeV. Radioisotope sources may require radiation shielding while not in use.

Pulse structure of neutron emission from isotopic source or reactor is usually controlled with a chopper system. Some reactors provide the pulse periodic operation mode. The neutron beam's energy follows ^{235}U fission spectrum distribution, or depends on the moderator type used inside the core or in neutron beam optics. Nuclear reactors are bulky, expensive, and require significant radiation shielding. That makes them impossible for use as a neutron source for portable material analysis systems.

Accelerator-based neutron sources are widely used in material analysis. These sources utilize charged particle beams to create fast neutrons in nuclear reactions induced in various targets. Some examples of such neutron producing reactions are the following: T(d,n)^{4}H, D(d,n)^{3}He, ^{9}Be(d,n)^{10}Be, ^{7}Li(d,n)^{8}Be, ^{7}Li(p,n)^{7}Be, ^{7}Be(p,n)^{7}B. The pulse neutron emission scheme allowing high repetition rates is provided by controlling acceleration parameters electronically. Such sources can be turned off thus simplifying radiation shielding requirements. The neutron sources based on fusion reactions are compact systems due to a large reaction resonance at low deuteron energy (approximately 3.4 barn for 100 keV for d-t fusion). The d-t fusion neutron generators are widely used as sources of neutrons for portable probe and industrial applications. These isotropic neutron sources are rugged, low maintenance, and relatively inexpensive systems.

2.1 Accelerator based fusion neutron generators

Neutron generators utilize d-t and d-d fusion reactions that produce mono energetic neutrons. The d-t reaction shows greater energy release. At the incident particle's small energies, ^{4}He and neutron share 17.59 MeV with conservation of linear momentum, and mono energetic 14.1 MeV neutrons are emitted out of reaction

$$^2\text{H} + {}^3\text{H} \rightarrow {}^4\text{He} + n \text{ (Q=17.59 MeV, } E_n\text{=14.1 MeV, } E_{He}\text{=3.49 MeV)} \tag{1}$$
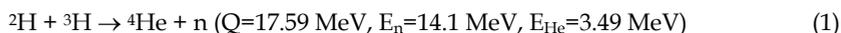
In 50% of events, d-d reaction produces mono energetic 2.45 MeV neutrons and ^{3}He that share 3.27 MeV:

$$^2\text{H} + {}^2\text{H} \rightarrow {}^3\text{He} + n \text{ (Q=3.27 MeV, } E_n\text{=2.45 MeV, } E_{He}\text{=0.82 MeV)} \tag{2}$$
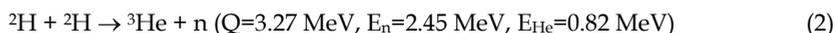
With 50% probability, ^{3}T and proton may be also produced in d-d reaction (Q=4.03 MeV, E_p=3.02 MeV, E_T=1.01 MeV).

Neutrons produced in the d-t reaction are emitted isotropically. Neutron emission in d-d reaction is slightly peaked forward along the direction of ion beam. The yield of d-d reaction at low energies of deuterons (reaction cross section is 3.3×10^{-2} barn at 100 keV) is approximately two orders of magnitude lower than in d-t fusion. Therefore, higher deuteron current is required to achieve d-d neutron yields comparable to a d-t source. Because of that d-t neutron generators are more common in applications requiring small size neutron sources of higher energy neutrons. The d-d systems may be preferable in applications where only the lower energy neutrons are required and where 14.1-MeV neutrons may cause unnecessary interference in the analysis due to many reactions channels open for high energy neutrons.

Another reaction which can be used for neutron production is the t-t fusion

$$^3\text{H} + {}^3\text{H} \rightarrow {}^4\text{He} + n + n \text{ (Q=11.3 MeV)} \tag{3}$$

The reaction cross section is 3.4×10^{-2} barn at 100 keV, which is similar to the cross section of the d-d reaction. The distribution of energy between reaction products varies producing the wide neutron spectrum with maximum energy up to ~11 MeV. Wide neutron spectrum may be useful for material analysis applications that require both low and high energy neutrons.

The compact "sealed tube" neutron generator design includes an ion source, a positive ion accelerator, and a target. Commonly used source to generate positive ions is the cold cathode Penning source. This source has a cylindrical anode under ~1-2 kV potential applied to it, and grounded cathodes on the ends of the anode. The magnet surrounds the anode cylinder setting up the coaxial magnetic field inside it. The tritium or deuterium gas is introduced into the volume of the anode cylinder. The electric field between anode and cathodes causes ionization of gas molecules creating the cold plasma. Trapped inside the anode electrons are moving in the volume and ionizing gas molecules which helps to maintain the plasma quality. Ions are transferred into the acceleration region through the exit port of the cathode. This region supplies the electric field (up to ~100-120 kV) to accelerate the positive ions. Neutron generator target is a metal hydride loaded with deuterium or tritium or the mixture of both. The ions interact with a target, producing neutrons in fusion reactions. Typical neutron output levels of sealed tube neutron generators are $~10^8$-10^9 n/s (d-t) and $~10^6$ n/s (d-d). Higher output usually shortens the sealed tube's life time. Sealed tube neutron generators are produced by Thermo Fisher Scientific, Schlumberger, Baker Hughes, EADS SODERN in France, and VNIIA in Russia.

Other designs of neutron generators utilize ion sources such as hot cathode source, radiofrequency ion source, or inertial electrostatic confinement (IEC) based source. For example, the pulse d-d system produced by Adelphi Technology Inc. (Williams et al., 2008) using the microwave driven plasma source technique provides the 2.45-MeV neutron output up to 8×10^9 n/s. The similar technique using tritium provides the yield of 14.1-MeV neutrons $~10^{11}$ n/s. The d-t neutron generator developed by NSD-Fusion GmbH for irradiation of extended samples uses the IEC technique producing $~10^{10}$ n/s. These neutron generator designs have the longer life time compared to sealed tube sources.

2.2 Gamma ray detectors

Physical parameters and limitations of the gamma ray detectors used in the system govern parameters of the entire system. The choice of gamma ray detectors is important for neutron based system to be effective. Improper solution can generate both false positive and false negative results.

The gamma ray detectors must be suitable for operation in mixed radiation fields where neutrons and gamma rays present. The detector material must have a high Z value to effectively detect characteristic photons with energies up to 10.8 MeV. The detection medium must also provide the energy resolution that allows resolving peaks of interest. Ideally, the detector should provide minimum interference with the signal emitted from a sample when the detector material is irradiated with neutrons. Thus, if possible the detector material should avoid isotopes that are anticipated in the analyzed samples. The neutron induced gamma ray peaks for elements of the detector material should not interfere with the sample's spectral signatures. In addition, neutrons may produce radioactive activation products with the time delayed decay inside the detector volume. These decays (for

example, the beta decay) may produce photons or charged particles that interfere with the characteristic gamma ray spectra adding the noise and overloading the data acquisition electronics. It is a complicated task to satisfy all these requirements, especially with added cost limitations. Usually, the trade-off between various detector parameters including its cost is considered for a particular application (Barzilov & Womble, 2006).

Standard gamma ray detector solutions for spectroscopy are high purity germanium detectors (HPGe) with liquid nitrogen dewar or mechanical cooling subsystems (Sangsingkeow et al., 2003), and scintillation detectors such as NaI(Tl), $Bi_4Ge_3O_{12}$, $LaBr_3$(Ce) (van Loef et al., 2001), etc. Noble gas scintillation or ionization detectors and gamma ray telescopes can also be used for neutron induced photon measurements in the MeV energy range (April et al., 2006).

The NaI(Tl) scintillator material has the light yield 38 photons/keV, 1/e decay time 250 ns, and density 3.67 g/cc. Atomic numbers are 53 and 11 for iodine and sodium, respectively. Under neutron irradiation, the NaI(Tl) scintillator is activated by neutrons showing the delayed beta decay spectral continuum with the endpoint energy ~2 MeV.

The BGO scintillator has the light yield 9 photons/keV, and 1/e decay time 300 ns. Due to the high atomic number of bismuth, 83, and the crystal's high density of 7.13 g/cc, the BGO scintillator is very effective for detection of high energy photons. Its energy resolution is lower than NaI(Tl) resolution: ~10% FWHM versus ~7% FWHM for 662-keV γ-rays. The BGO demonstrates excellent behaviour under neutron irradiation without delayed decay issues. Significant downside of the BGO detector is its sensitivity to the environmental temperature (Womble et al., 2002).

The $LaBr_3$(Ce) scintillator has the ~3%-resolution of the 662-keV peak, and density 5.08 g/cc. The lanthanum atomic number is 57. This scintillator has high light yield 63 photons/keV, fast 1/e decay time 16 ns, and better timing properties than NaI(Tl). The $LaBr_3$(Ce) material contains small quantities of the radioactive lanthanum-138 isotope ($t_{1/2}$=1.02×10^{11} years) producing the 1.47-MeV gamma ray peak that is always visible in the spectrum; it can be used for calibration purposes. The $LaBr_3$(Ce) is affected by neutrons showing the delayed beta decay spectral continuum with endpoint energy ~3 MeV when irradiated with a d-t neutron source. The measured β-decay curve exhibits cumulative nature: two isotopes decay at the same time. The ^{80}Br decays with a half-life 17.68 minutes. The ^{82}Br isotope decays with the half-life approximately 35 hours. Lanthanum halide demonstrates stable gamma ray spectrum parameters in the mixed field under d-t neutron irradiation, when properly shielded. The good energy resolution under the room temperature, the high brightness, and the high scintillation decay speed pose this material as a promising candidate for active neutron interrogation applications, if the crystal's neutron activation issues are properly addressed.

The HPGe detector has superior energy resolution comparing to scintillation detectors. The atomic number of germanium is 32. The HPGe crystal density is 5.35 g/cc. HPGe crystal is sensitive to the high energy neutrons, which cause detector damage (Tsoulfanidis & Landsberger, 2010). High energy neutrons produce charges in the germanium crystal which are adding noise to the collected gamma ray spectrum (Ljungvall & Nyberg, 2005). Neutron collisions with the crystal cause atom displacements into interstitial positions creating a vacancy pair. These crystal defects behave as trapping

centers for holes and electrons, and may create new donor and acceptor states, thus gradually changing the charge collection efficiency, the resolution, and the pulse timing characteristics of the detector. The n-type HPGe detectors are preferable in applications that involve neutron irradiation. They have been shown to be more resistant to damage by fast neutrons (Pehl et al., 1979). The neutron damage problem requires special attention and treatment (Fourches et al., 1991). The speed of the HPGe charge collection is another parameter to be considered in high count rate conditions and applications that require good timing resolution (Cooper & Koltick, 2001).

The comparison of selected gamma ray detectors used in neutron-based material analysis applications is shown in Table 1.

The shielding is required to protect the gamma ray detector from direct hit by the neutrons. Shielding size defines the geometry of the system since a neutron source and a gamma ray detector are separated by the shielding column. The combination of materials with large scattering cross sections for fast neutrons and large low energy neutron capture cross sections, and high Z materials with high stopping power for gamma rays is used. The goal is to keep fast neutrons away from the detector volume either by redirecting their path or moderating them with the subsequent capture. The d-d or d-t targets are in general of the "point source" type, thus the shielding may have a conical shape to minimize the weight. For 10^8-n/s d-t source, the simplest "shadow" shielding is a layered conical structure of ~50 cm length; the 30-40 cm borated polyethylene layer near the source, and the 10-20 cm lead layer near the gamma ray detector (Womble et al., 2003). The more complex shielding designs are possible using layers of other materials, but the size / weight / cost considerations add design limitations. In addition, the detector may be also shielded from lower energy neutrons scattered from surrounding materials. The two-layer shielding can reduce spectral noise due to low energy neutron interactions with the detector crystal. The outer layer of borated resin is effective as a thermal neutron shielding; the inner lead layer attenuates photons emitted from thermal neutron capture reactions in the outer layer. The lead also attenuates low energy photons that are not of interest in material analysis thus helping to reduce dead time of the gamma ray spectroscopy system.

Detector	Energy resolution, %FWHM @ 662 keV	Efficiency	Cooling	Neutron activation issues
NaI(Tl)	~7% Fair	Medium	No	Activated, beta-decay
$Bi_4Ge_3O_{12}$	~10% Fair	High	No, temp. shifts	No
LaBr$_3$(Ce)	2.8% Good	Medium	No	Activated, beta-decay
HPGe	0.4% Excellent	Medium	LN$_2$ Temp.	No

Table 1. Gamma ray detectors used in neutron-based material analysis applications

Data acquisition electronics used with the gamma ray detectors in such systems should be appropriate for the detector's signal processing and count rates attainable in neutron interrogation. Standard analog and digital spectroscopy solutions are typically used.

3. Nuclear reactions induced by neutrons

Neutrons emitted in d-d (E_n=2.45 MeV) and d-t (E_n=14.1 MeV) fusion reactions are highly penetrating particles. The typical range is several feet into materials commonly utilized in industry and commerce. Nuclear reactions energetically possible under 14.1-MeV fusion neutron's action in the volume of the irradiated object are the following: (n,n'γ), (n,γ), (n,α), (n,p), (n,d), (n,t), (n,2p), (n,n'p), (n,n'α), (n,³He), and (n,2n). If the sample contains heavy nuclei, (n,3n) and nuclear fission reactions may be induced with the low probability. Production of charged particles is prevailing for light nuclei; neutron production is favourable for heavier nuclei. The reactions (n,d) and (n,t) have noticeable cross-section for light mass isotopes, but products produced in such reactions are stable. The (n,d) and (n,t) reaction cross sections for medium and heavier mass nuclei are low.

Widely used in material analysis neutron induced nuclear reactions are inelastic neutron scattering (n,n'γ), thermal neutron capture (n,γ), and neutron activation (n,αγ) and (n,pγ). The only source of fast neutrons is a fusion neutron source. Thermal neutrons are created by slowing down the fast source neutrons in collisions with low Z materials within the sample itself or within the environment around the sample, or by using neutron moderating materials.

Isotope	σ_{total}	σ_{inl}	$\sigma_{n\text{-}n'\ 1st}$	$\sigma_{n\text{-}n'\ 2nd}$	$\sigma_{n\text{-}n'\ 3rd}$	$\sigma_{n,\alpha}$	$\sigma_{n,p}$
¹H	692.0	0.0	0.0	0.0	0.0	0.0	0.0
¹²C	1303.2	426.9	184.7	0.9	9.9	72.7	0.2
¹⁴N	1628.6	399.3	14.9	26.7	15.3	60.1	54.0
¹⁶O	1611.1	508.5	27.0	82.5	43.0	109.0	43.7
¹⁹F	1740.7	164.2	0.3	36.8	0.3	21.3	14.7
³¹P	1831.7	53.9	0.2	0.2	0.1	126.9	91.9
³²S	1829.7	378.9	99.3	10.3	18.0	159.6	247.4
³⁵Cl	2100.0	820.0	5.8	5.2	12.0	137.3	98.0
⁷⁵As	3456.2	685.1	0.8	0.5	7.3	10.1	19.0

Table 2. 14.1-MeV neutron induced nuclear reaction cross sections (in millibarns): σ_{tot} – the total neutron cross-section; σ_{inl} – the inelastic neutron cross-section; $\sigma_{n\text{-}n'\ 1st\ level}$ – the (n,n') cross-section which excites the nucleons to the first nuclear level; $\sigma_{n\text{-}n'\ 2nd\ level}$ – the (n,n') cross-section which excites the nucleons to the second nuclear level; $\sigma_{n\text{-}n'\ 3rd\ level}$ – the (n,n') cross-section which excites the nucleons to the third nuclear level; $\sigma_{n,\alpha}$– the (n,α) cross-section; and $\sigma_{n,p}$ – the (n,p) cross-section

Isotope	σ_{total}	σ_{inl}	$\sigma_{n\text{-}n'\ 1st}$	$\sigma_{n\text{-}n'\ 2nd}$	$\sigma_{n\text{-}n'\ 3rd}$	$\sigma_{n,\alpha}$	$\sigma_{n,p}$
¹H	2683.6	0.0	0.0	0.0	0.0	0.0	0.0
¹²C	1595.3	0.0	0.0	0.0	0.0	0.0	0.0
¹⁴N	1512.6	0.0	0.0	0.0	0.0	70.2	22.4
¹⁶O	561.4	0.0	0.0	0.0	0.0	0.0	0.0
¹⁹F	2763.5	995.3	246.3	346.8	99.4	0.01	0.0
³¹P	3036.1	448.3	448.3	0.0	0.0	0.0	30.8
³²S	3422.6	6.9	0.0	0.0	0.0	129.9	58.2
³⁵Cl	3050.4	428.3	124.4	243.9	0.0	4.1	32.0
⁷⁵As	3238.3	1728.5	37.0	60.0	78.4	0.0	0.02

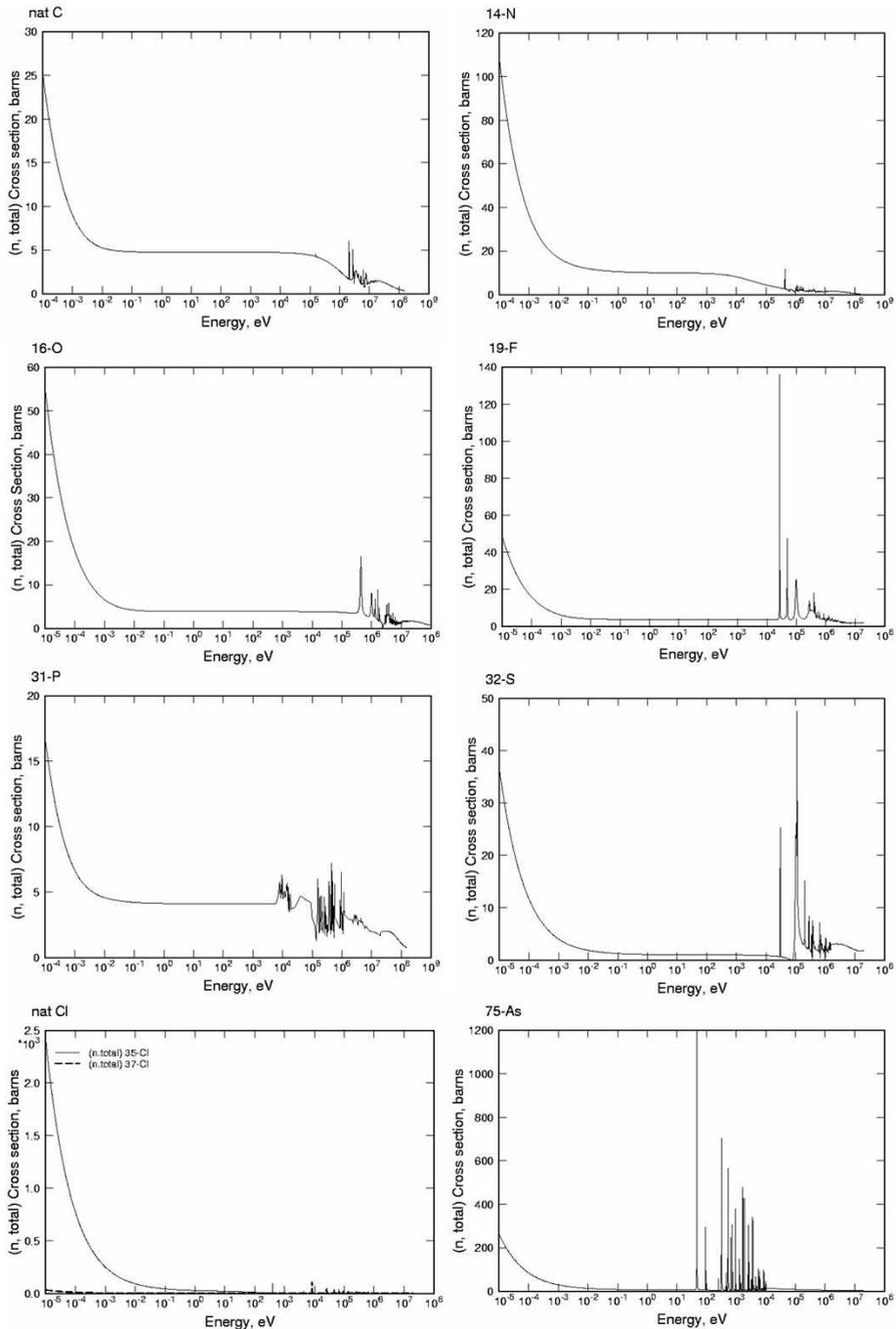Table 3. 2.45-MeV neutron induced nuclear reaction cross sections (in millibarns)

Fig. 2. Neutron cross sections (n, total) for C, N, O, F, P, S, Cl, and As

Isotope	^{1}H	^{12}C	^{14}N	^{16}O	^{19}F	^{31}P	^{32}S	^{35}Cl	^{75}As
σ_{th}	332.7	3.5	79.8	0.2	9.7	172.7	548.1	33070.2	4528.3

Table 4. Thermal neutron capture reaction cross sections at E_n=0.025 eV (in millibarns)

The representative set of elements (H, C, N, O, F, P, S, Cl, and As) is selected as an example of isotopes found in explosive, chemical threats, coal and other materials. The parameters of the d-t neutron induced nuclear reactions are shown in Table 2. Table 3 shows the d-d neutron induced nuclear reactions at E_n=2.45 MeV for the same set of elements. The (n,γ) thermal neutron capture reaction's cross-section at E_n=0.025 eV are shown in Table 4. The total neutron cross-sections σ_{tot} for C, N, O, F, P, S, Cl, and As are shown in Fig.2. The neutron data for other isotopes are available from website of the Nuclear Information Service of the Los Alamos National Laboratory at http://t2.lanl.gov/data/data.html.

The (n,2n) reaction is also utilized to produce the excited energy states causing the delayed beta decay with associated photon emission that may be non-fingerprint in nature, but it may assist to identify the amount of a parent isotope in the sample. The fast neutron activation of this type can be used for example to measure amount of nitrogen in a sample via reaction ^{14}N(n,2n)^{13}N. The produced ^{13}N isotope has $t_{1/2}$=10.1 minutes emitting positrons. They annihilate immediately with electrons in the sample matrix emitting 511 keV gamma rays. Although it is not characteristic photon energy, it indicates the presence of a positron emitter. If measured correctly in time and associated with $t_{1/2}$ of ^{13}N isotope, this signature can be used in material analysis. The issue of such approach is the possibility of the beta annihilation photon's emission by other ^{13}N-producing parent nuclei. For example, elements that may cause neutron based production of ^{13}N are boron and oxygen. The 1.47-MeV alpha particles may be initiated by thermal neutrons via ^{10}B(n,α)^{7}Li reaction, producing 511-keV photons through the ^{10}B(α,n)^{13}N reaction. Knockout protons of high energy produced by fast neutrons may initiate the 5.5-MeV-threshold ^{16}O(p,α)^{13}N reaction. The ^{63}Cu(n,2n)^{62}Cu reaction can produce the positron emitter ^{62}Cu → ^{62}Ni + e$^+$ ($t_{1/2}$=9.8 minutes). So, the 511-keV annihilation photons emitted from copper and nitrogen nuclei have a close half-life values. Thus the use of other gamma ray signatures utilizing other reactions in conjunction with the positron annihilation would be beneficial in the material analysis.

4. Characteristic gamma radiation

As a result of nuclear reactions involving the isotopes contained in the object under scrutiny, exited nuclei emit gamma rays with specific energies in the de-excitation process. They act as the "fingerprints" of these isotopes. Most γ-rays are emitted promptly after the reaction. The "prompt" photon emission from excited nucleus occurs within approximately 10^{-9} seconds after initial excitation. However, in some cases, a nucleus with a half-life of a few seconds to a couple of minutes is formed. This radioactive nucleus decays to a daughter nucleus emitting various particles (α, β^+, β^-, etc.) and delayed photons. The prompt gamma ray emission occurs either in the single transition as it happens in the case of hydrogen 2.223-MeV gamma rays, or through several transitions emitting many prompt γ-rays of lower energy. The examples of energy level schemes for ^{12}C and ^{16}O nuclei are shown in Fig.3.
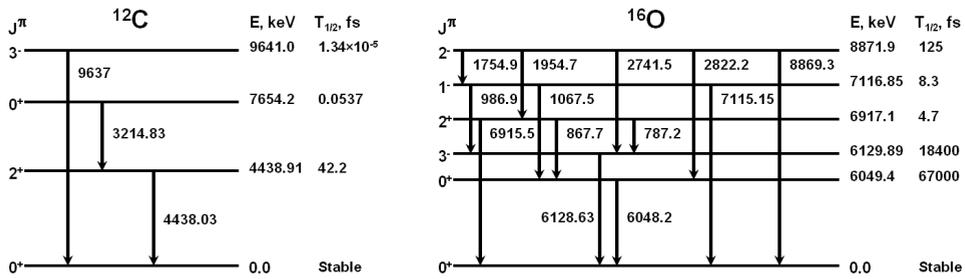
Fig. 3. Energy level schemes for ^{12}C and ^{16}O

Isotope	Reaction	E_γ, keV
^{1}H	(n,γ)	2223
^{12}C	(n,n$'\gamma$)	4438
^{14}N	(n,n$'\gamma$)	730, 1634, 2313
	(n,γ)	1885, 5269, 5298, 10829, 10318
^{16}O	(n,n$'\gamma$)	5618, 6129
^{19}F	(n,n$'\gamma$)	197, 1236, 1348, 1357
	(n,γ)	582, 2453, 3589
^{31}P	(n,n$'\gamma$)	1266, 2028, 2233
	(n,γ)	636, 2154, 3900, 6785
^{32}S	(n,n$'\gamma$)	1273, 2230
	(n,γ)	841, 2380, 3221, 5420
^{35}Cl	(n,γ)	788, 1165, 1951, 1959, 6111, 7414
^{75}As	(n,n$'\gamma$)	199, 265, 280, 573
	(n,γ)	165, 472, 1534, 6810

Table 5. Characteristic gamma rays

The intensities of the obtained specific gamma rays provide information about the number of atoms in the sample. Hence, the information on its chemical composition can be extracted from the measured gamma ray spectrum. The list of isotopes, nuclear reactions, and energies of most prominent characteristic gamma rays are shown in Table 5. Emitted due to neutron induced reactions photons are highly penetrating. For example, energy of gamma rays emitted from nuclear reactions on nuclei of carbon, oxygen, and nitrogen isotopes is between 4 and 11 MeV. Table 5 is not inclusive. The prompt gamma rays for other elements can be found in the following libraries. The prompt gamma rays from thermal neutron captures (n,γ) are catalogued in the library for natural elements (Lone et al., 1981). It lists the prompt gamma ray energies in the range from 23 keV to 10829 keV for all isotopes, in terms of gamma rays emitted per 100 neutron radiative captures. These data are also available online from the National Nuclear Data Center (Brookhaven National Laboratory) at http://www.nndc.bnl.gov/capgam/. Zhou Chunmei compiled the thermal neutron capture data for nuclides with A>190 (Chunmei, 2001) and new evaluation data for thermal neutron capture for elements A=1-25: level properties, prompt gamma rays, and decay scheme properties (Chunmei, 2000). The experimental data on the (n,n$'\gamma$) photons are compiled by

Demidov and colleagues in the IAEA document INDC-CCP-120 (Demidov et al., 1978). The gamma ray spectra from inelastic scattering were measured for all elements except unstable isotopes and noble gases.

The gamma spectrum obtained from ammonium nitrate sample irradiated with a d-t source is shown in Fig.4. Spectrum was measured using HPGe detector. We would like to note the spectral feature of Doppler broadening that is specific for photons induced by 14.1-MeV neutrons on light nuclei. The two inset expanded spectra in Fig.4 show the gamma ray from $^{12}C(n,n'\gamma)^{12}C$, 4.438 MeV and $^{16}O(n,n'\gamma)^{16}O$, 6.13 MeV. It is readily apparent that the gamma ray peak from ^{12}C is much wider than the gamma ray peak from ^{16}O. Other causes of this widening such as electronic noise, crystal damage due to neutron irradiation can be dismissed since ^{16}O does not have any evidence of the broadening. The broadening of the gamma ray peaks for light nuclei was studied in (Womble et al., 2009). The energy levels of the nucleus have different spins and parities, and the state's life times. For example, in ^{16}O, the 2nd excited state with the energy of 6.13 MeV has a half-life of 18.4 ps (see Fig.3). The 3rd excited state has a half-life nearly 2000 times shorter (8.3 fs). Energies of these two states are close to each other, but the 2nd excited state to ground state transition is $3^- \to 0^+$ and the 3rd excited state to ground state transition is $2^+ \to 0^+$. Thus the difference in half-life is due to the transition probability of producing E3 radiation versus E2 radiation. The half-life time of 4.43-MeV level in ^{12}C is 42 fs. Carbon and oxygen nuclei recoiling in inelastic neutron scattering reactions under 14.1-MeV neutrons have similar stopping times moving in the matrix of the sample; for example, approximately 1800 fs for the NH_4NO_3 sample. Therefore ^{12}C nucleus may emit photon while in motion exhibiting the Doppler broadening effect for the 4.43-MeV peak, but ^{16}O nucleus is stopped before the emission of the 6.13-MeV gamma ray and therefore does not experience the peak broadening in the measured spectrum.
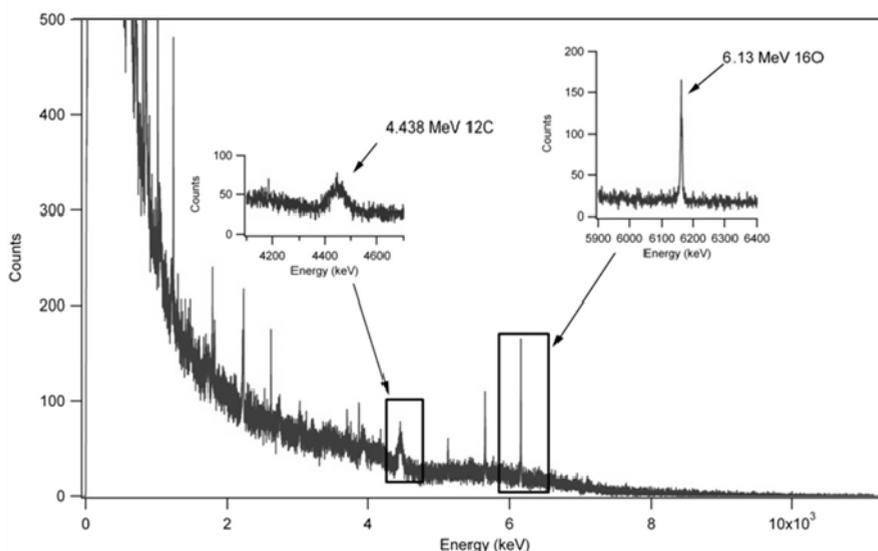

Fig. 4. d-t neutron induced gamma ray spectrum for ammonium nitrate

5. Methods and applications

This section covers a number of systems that perform bulk material analysis using neutron induced gamma spectroscopy. Although this is by no means a complete list, it represents systems and techniques that have been utilized in the past twenty years. Some of these systems are still in the market and some never made it to market. Some of the systems have different acronyms or different trade names but rely on the same physical principles:

- PGNAA - Prompt Gamma Neutron Activation Analysis
- PFNA - Pulsed Fast Neutron Analysis
- PFTNA - Pulsed Fast/Thermal Neutron Analysis
- PFNTS - Pulsed Fast Neutron Transmission Spectroscopy
- API – Associated Particle Imaging

5.1 Prompt gamma neutron activation analysis

Admittedly, Prompt Gamma Neutron Activation Analysis (PGNAA) is usually thought of as a continuous (or DC) source technique. In this technique, fast neutrons from a radioisotope, a neutron generator or a reactor impinge upon a sample. The sample then emits gamma rays through (1) prompt gamma ray emission from gamma decay, (2) gamma ray emission through short-lived beta decay, or (3) prompt gamma ray emission due to exoergic nuclear reactions. By the latter, we mean gamma ray emission to satisfy conservation of energy (or mass) in a nuclear reaction. The most well-known gamma rays from this type of reaction are the 2.22 MeV gamma ray from the $^1H(n,\gamma)$ reaction and the 10.8 MeV gamma ray from the $^{14}N(n,\gamma)$ reaction.

Pulsed neutron sources can be used in PGNAA systems. However, using pulsing neutron generators without taking advantage of the pulsing mechanism is not efficient.

5.2 Pulse fast neutron analysis

Tsahi Gozani, Peter Sawa, and Peter Ryge conceived of Pulsed Fast Neutron Analysis (PFNA) in 1987 while they were working at SAIC (Gozani, 1995). In PFNA, a large accelerator creates a deuteron beam which is directed at a deuterium gas target. A chopper, which consists of strong electric field that periodically sweeps the deuteron beam away from the target, creates neutron pulses of a few nanoseconds duration. In described system, user has control of the chopper, so moment when neutrons are created and duration of the neutron pulse are known precisely. The PFNA uses time-of-flight (TOF) methods to obtain a favourable signal-to-noise ratio (SNR) to detect various chemicals. The accelerator used in PFNA is typically an 8 MV Van de Graff accelerator. The D(d,n) reaction has a low Q-value (approximately 100 keV). Thus any energy above the Q-value is mostly transferred to the kinetic energy of the neutron, producing a neutron with a maximum kinetic energy of 8 MeV. The velocity of 8 MeV neutrons is about 6 cm/ns. The user, then, knows exactly when the neutron pulse is made and now can estimate its position at any time after its creation.

Furthermore, due to the high kinetic energy of the deuteron beam, the neutron's momentum is parallel to the momentum of the deuteron. The developers took advantage of this fact and used a sophisticated system to "raster" the neutron beam across the object of interest. The

neutron beam also has a small angular divergence and estimates (Strellis, 2009) are that the beam is 9 cm × 12 cm in the center of the object of interest.

PFNA systems can be used to screen very large cargo shipments such as tractor-trailer shipping containers and airport shipping containers. A large, 2-dimensional array of NaI gamma ray detectors covers the cross-section area of the object under scrutiny.

The energies of the gamma rays emitted from the object are plotted against the TOF of the neutron. This creates a two-dimensional array of data that looks similar to a spectrogram in that the intensity of the gamma ray at a particular TOF is represented by a color using the RGB color scheme. In this array of data, color bands parallel to the TOF axis indicate constant gamma ray background such as from normally occurring radioactive materials (NORM). Color bands parallel to the energy axis represent the gamma ray spectra of volume elements ("voxels") within the object of interest. The volume element size is based on the time resolution of the system so the voxels are approximately 5-cm thick. For example, in the center of the container the voxel is 9 cm × 12 cm × 5 cm. The small voxel size increases the SNR of the system. Another benefit is that the lifetime of certain activation products can be measured and this gives more data upon which to identify the material.

At early development stage, price and size were the drawbacks of using PFNA. However, since the 9/11 attacks the main challenge is the system cost. The cost includes installation and maintenance of this complex system. In 2009, there was a single system working at the George Bush Intercontinental Airport (Strellis, 2009). As of this writing, we are aware of no other installations.

5.3 Pulsed fast / thermal neutron analysis

The Pulsed Fast/Thermal Neutron Analysis (PFTNA) is a technique used in conjunction with small, portable electronic neutron generators. It was originally developed by George Vourvopoulos, Phillip Womble, and Frederick Schultz and presented in (Womble et al., 1995). Unlike PFNA, which has pulse duration of approximately 2 ns, PFTNA employs pulses with a minimum duration of 5 μs. Longer pulse duration significantly reduces cost of PFTNA systems. The PFNA system can be used in a "macro-pulse" mode, in which the neutron beam is turned off for a period of 100 μs. This "macro-pulse" mode mimics the PFTNA system's mode.

The advantage of the PFTNA systems is an ability to separate the gamma ray spectrum of inelastic scattering reactions (n,n'γ) from thermal neutron capture (n,γ) and activation reactions (e.g. (n,p)) gamma-ray spectra. The data acquisition system collects data during the neutron pulse at one memory address and then switches to another memory address to acquire data between pulses. The data collected during the pulse is primarily from (n,n'γ) reactions and the data collected between pulses is primarily from (n,γ) reactions. Often systems are designed to be shut off for a few minutes to collect short-lived activation products such as $^{16}O(n,p)$ ($t_{1/2} \approx 16$ s). It is a common misconception that the frequency and duration of the neutron pulses is chosen to maximize the data from the (n,n'γ) reactions. In fact these parameters are chosen to maximize the (n,γ) reactions or more precisely the thermal neutron flux. The neutron pulse frequency determines whether the thermal neutron flux is kept near constant or if it is allowed to diffuse. Applications such as differential die-

away analysis (DDA), a method of measuring fissile content, allow the thermal neutron flux to completely diffuse and use pulse frequencies less than 1 kHz. PFTNA systems use pulse frequencies greater than 5 kHz to ensure that the thermal neutron flux is nearly constant for the entire period of measurement (Vourvopoulos & Womble, 2001). Our personal experience in this area has shown that frequencies higher than 10 KHz may be desirable as well.

For a d-t or d-d neutron generator, the typical pulsing method is to clamp the so-called source voltage using "clamping circuits". The source voltage causes ionization of the deuterium gas before the ions are accelerated. A consequence of the higher pulse frequency is the shorter pulse duration. This is due to the fact that these clamping circuits operate at a constant duty cycle. The source voltage duration must be a few microseconds (approximately 4 µs) for the deuterium gas to reach a pressure where ionization occurs (the "fill time"). With this condition along with the constant duty cycle, the maximum neutron pulse frequency is about 20 kHz since higher frequencies (>25 kHz) will not have a sufficiently long fill time. Thus PFTNA pulses are typically 10 µs in duration with a pulsing frequency of 10 kHz. The PFTNA scheme with the neutron pulse's time structure is shown in Fig.5.
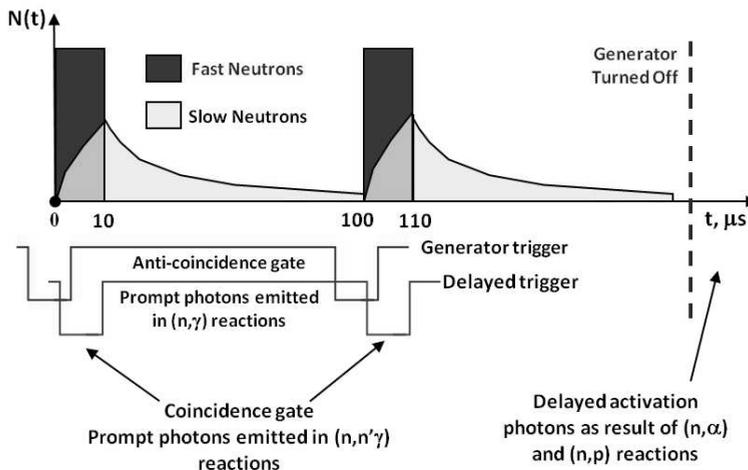

Fig. 5. Pulse fast thermal neutron analysis scheme

As discussed earlier, PFTNA method uses two different memory addresses depending whether the neutron generator is on or off. The use of two memory addresses is sometimes described as "ping-ponging" since the data "bounces" between two addresses. A gate signal is sent from the neutron generator to the data acquisition to indicate whether the generator is on or off. The gate signal is usually delayed from the rise of the source voltage by the fill-time. Furthermore the gate signal will extend past the fall-time of the source voltage by a few microseconds. This lag is due to the processing time of the data acquisition system. One of the reasons that PFTNA systems use fast data acquisition electronics is to minimize this lag.

Another reason to use fast data acquisition electronics in PFTNA systems is high counting rate in the detector when the neutron generator is producing neutrons. Data acquisition rates in the system during this period can exceed 100 kcps. High rates such as these can overwhelm HPGe detectors and analog amplifies. Modern digital electronics can cope with these rates but as rates approach 1 Mcps, scintillation detectors such as sodium iodide or bismuth germanate can be overwhelmed. Count rate limitations force PFTNA system designers to place shielding material between the detector and the neutron generator that adds to system weight.

The d-d and d-t fusion reactions take place at low momentum which means that the neutrons are emitted isotropically. These systems typically consume about 100 W during operation. The average neutron outputs for PFTNA systems are 10^8 n/s for d-t based systems and 10^6 n/s for d-d based systems. For d-t systems, this leads to radiological concerns to personnel which can be mitigated by distance (approximately 8 meters stand-off for unshielded operation) or shielding (approximately 30-50 cm shielding).

The benefits of PFTNA systems are their smaller size and relatively low cost. However, these features lead to a lower SNR compared to PFNA systems. Some research teams have suggested combining PFTNA method with the associated particle imaging technique to improve the SNR.

5.4 Associated particle imaging

In associated particle imaging (API), the recoiling residual nucleus, e.g. the alpha particle for d-t reaction, is used to perform time-of-flight and direction selectivity. SNR could be greatly improved for (n,n'γ) gamma ray spectra by measuring gamma ray signals that are emitted only from the selected volume. However, application of this technique would have no effect on the SNR of the (n,γ) or the time delayed activation gamma ray spectra.

The scheme of API technique is shown in Fig.6. The d-t fusion reaction produces alpha particle and 14.1-MeV fast neutron that are emitted in opposite directions due to linear momentum conservation. The segmented alpha detector installed inside the sealed neutron generator tube is used for detection of the α-particle event's position and time to "tag" the direction of the 14.1-MeV neutron (Koltick et al., 2009). The geometry of segments of the alpha detector and the neutron's times-of-flight define the geometry of "voxels" for the 3D analysis. ZnO(Ga) detector was used as an alpha detector. It was found that detector's efficiency is about 90% for 3.49-MeV alpha particles. The phosphor coating emits ~15 photoelectrons / alpha; its scintillation emission peaks at 390 nm with ~3.3-ns decay time, allowing up to ~2×10^{10} n/s output for 2% tagged solid angle without significant pile-up (Cooper et al., 2003).

The alpha particle detection event and gamma ray detection event are both stamped with the timing signals. The DAQ system is set up to produce the logic signal when both events (the alpha particle and the photon detection) are recorded within a short time interval – the "coincidence window". This logic signal is used to select those gamma ray signals in the energy spectrum that arrive from the tagged voxel. The 14.1-MeV neutron travels in air with the velocity ~5 cm/ns. The 3.49-MeV α-particle has the velocity ~1.3 cm/ns. Thus the coincidence window should be in the order of nanoseconds. The quality of the timing

signals for both detectors should be very high, without jitter. The width of the coincidence window and the neutron flux are interconnected: the random coincidence rate increases with the higher neutron flux thus limiting neutron yield of the generator.

The API technique was used in such systems as SENNA (Vakhtin et al., 2006), EURITRACK (Perret et al., 2006), and UNCOSS (Eleon et al., 2010).
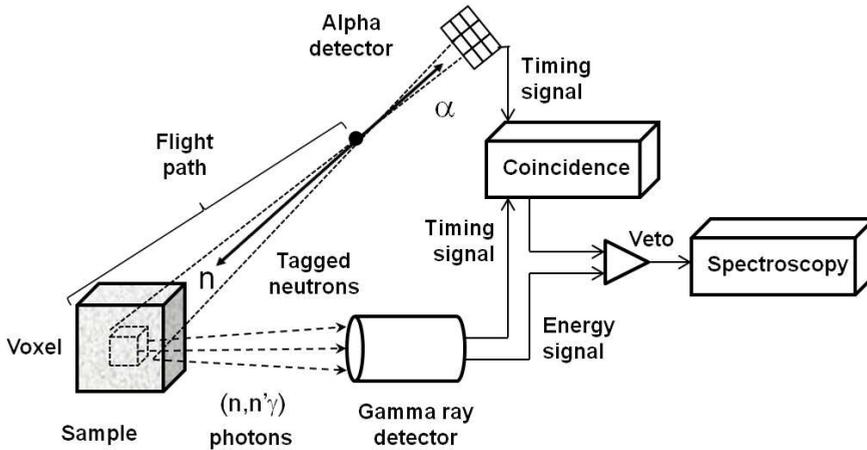

Fig. 6. Associated particle imaging technique

5.5 Pulsed fast neutron transmission spectroscopy

Pulsed fast neutron transmission spectroscopy (PFTNS) is the only technique in this section, which examines the resulting neutron spectrum, instead of the gamma ray spectrum. In this technique, a broad energy beam of neutrons is directed at an array of neutron detectors. The object under interrogation is passed through the beam and the resulting attenuated neutron spectrum is measured using the neutron detectors. This method is the same method that researchers use to perform neutron cross-section measurements.

The pulsing in PFTNS allows the system to perform neutron TOF measurements. These TOF measurements are used to determine the energy of the neutrons with flight paths of 4 to 10 m. The resulting neutron spectrum is used to estimate the attenuation of neutrons as function of energy. Light elements such as H, C, N, and O have high cross-sections for neutron attenuation at these energies. Thus the relative amounts of H, C, N, and O can be determined, and the "imaging" of elements is possible. The voxel sizes would be similar to those of PFNA due to the limits of the speed of the neutrons.

Due to the high neutron fluences and precise timing required for PFTNS, this system needs an accelerator similar to the one utilized by PFNA. The TOF path means that the systems take a large amount of space. These are two of the reasons that these systems were not widely adopted by the security community.

PFTNS was proposed as a primary or secondary screening system for airline security. Designs were proposed which would handle a large number of bags per minute. This would be achieved by having the bags ride a carousel around accelerator. The neutron detectors would be placed in a "wall configuration" and the neutron beam would raster through a number of bags. The National Academy report (NNMAB-482-6, 1999), written in 1999, was extremely critical of the utilization of PFTNS for airport security. However, Overley suggests that detection rates of 93% and false alarm rates of 4% are possible with this technique (Overley et al., 2006).

6. Gamma radiation spectral analysis

Neutron based material analysis methods generally require a skilled analyst to interpret the gamma ray spectral data collected, and to classify the interrogated object using the elemental parameters extracted from the spectral data. Automatic spectral analysis algorithms and the object's classification algorithms are required for real world applications where access to nuclear spectroscopy expertise is limited, or the autonomous and/or the robotic operation is necessary.

6.1 Analysis of neutron induced gamma ray spectra

The first step in the data analysis process is to extract the sample's elemental information from the measured gamma ray spectra. The spectrum analysis algorithms that are used for that purpose should simultaneously provide quick, accurate, and objective analysis of gamma ray spectra by evaluating the intensities of the characteristic photon peaks. For spectra measured with high resolution detectors such as HPGe, the approach can be based on the peak finding algorithm using the regions of interest (ROIs). Usually, the "blank" spectrum (measured with no sample present) is subtracted from the "sample" spectrum (measured with the sample) before the spectral analysis. It takes into account the signatures of the same elements that are present in surrounding materials, and in the sample. The "nuclear" ROI parameters such as the net peak area in counts /second units are proportional to the number of isotopes in the sample that emitted the fingerprint gamma rays. The "nuclear" parameters may be converted into other appropriate units, if needed, using the elemental calibration library (for example, "chemical" parameters accepted in the coal or the cement analysis industry, etc.). These libraries are created for the system using calibration measurements using known samples.

The simple ROI-based method may be appropriate for non-complicated spectra with the peaks that are well resolved. For spectra with many closely positioned peaks, or low resolution spectra with overlapping peaks, the peak-shape fitting algorithms are required. The mathematical method of measured spectrum fitting as the linear combination of single element's detector responses, that are measured experimentally, was developed by George Vourvopoulos and Phillip Womble (Vourvopoulos & Womble, 2001). To use this method, one must first measure the response of the low resolution detector to γ-rays from pure elements. For example, a block of pure graphite is used to determine the detector's elemental response to the carbon γ-rays. To determine the detector's elemental response to hydrogen, a response is measured from a water sample, and so on. The counts in i-th channel of the spectrum of a sample S can be represented by the equation:

$$S_i = K \cdot BL_i + \sum_{j=1}^{m} A_j \cdot RF_{i,j} \tag{4}$$

Here: BL_i is the blank spectrum at the i-th channel and K is its coefficient; $RF_{i,j}$ is the detector's elemental response of the j-th element at the i-th channel and A_j is its coefficient, and m is the total number of elements used for this spectrum decomposition procedure. The coefficients K and A_j are found by the least squares algorithm minimizing the χ^2 to find the "best fit". As the result of this decomposition procedure, the intensities of peaks of j elements used in this fitting are found in counts / second.

Another spectral decomposition technique developed by Robin Gardner and colleagues (Shyu et al., 1993) utilizes the detector's elemental responses that are calculated using Monte Carlo methods. The experimental method of detector's elemental response generation provides detailed realistic spectral features (i.e. electronics noise, peak broadening, neutron activation effects, etc.), but it is time intensive, and the set of pure element samples may be limited. The computational method allows generation of responses for the larger set of elements, but it may be problematic to represent detailed spectral features because not all processes in a Monte Carlo code may be taken into account.

Bruce Kessler applied the original mathematical method based on multi-wavelets to analyze the neutron induced photon spectra (Kessler, 2010). In this approach, the set of special scaling vector components was developed for spectrum fitting. Wavelet decompositions ignore signal components up to the approximation space of the basis, so the wavelet analysis is used to look for patterns over the top of spectral "noise". The measured sample spectrum wavelets are decomposed using a variable linear combination of the wavelets from the decompositions of detector's elemental responses providing the intensities of characteristic gamma ray peaks. The algorithm was shown to be effective for both high resolution and low resolution spectra.

6.2 Classification algorithms

The object's classification algorithms are responsible for material identification using the characteristic gamma ray peak data that are produced by the spectral analysis algorithms. The classification uses the fact that the amount of particular isotopes varies for different materials (i.e. based on their chemical formula, taking the reaction cross sections into account).

The suitable approach is to represent the measurement result as a "point" in the space of several parameters (elemental intensities). Different materials containing the same isotopes but in different ratios are represented by points that are segregated in such "elemental" space. The dimension of this space is determined by the number of isotopes.

In general, the "nuclear" data obtained with neutron based systems differ from elemental composition evaluations based on chemical formula due to several reasons such as statistical nature of nuclear reactions, short measurement times, presence of radiation shielding, and other environmental conditions. Thus, the chemical compound measured in various conditions is represented not by the single "point" in the elemental space, but rather by a cloud-like set of points, where each point corresponds to one measurement.

Clouds have circular structure, and create specific patterns for classes of different materials. Fig. 7 shows a two-dimensional slice of the elemental space. It represents two isotopes: oxygen and nitrogen. Four materials that contain different amounts of oxygen and nitrogen were used as samples for measurements in various environmental conditions. The (nitrogen, oxygen) points from many measurements shape the 2D clouds on the figure.

The classification decision is made using the boundaries calculated to separate these classes. For the well separated clouds, the boundaries can be found easily, and simple decision making logic "trees" can be constructed. But in many cases, the patterns for threats and innocuous materials are overlapped in the multidimensional space of parameters making the differentiation task challenging for classical decision-tree algorithms.
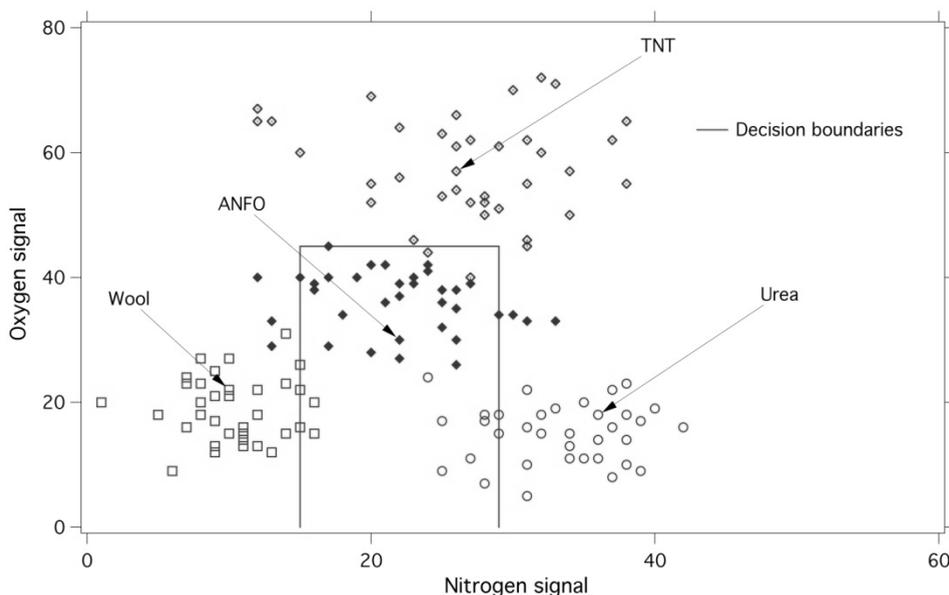
Fig. 7. Data points for four different substances

The decision-tree algorithm for the identification of the particular threat material ("ANFO") amongst four classes of materials is shown in Fig.8. It can be described as the following: if detected oxygen signal lies between lower and higher thresholds, then nitrogen signal is checked. If nitrogen signal lies between lower and higher thresholds, then substance can be identified as "ANFO". The thresholds in the decision tree (N_{low}, N_{high}, O_{high}) can be varied in order to achieve better results. Each threshold value can be represented as a horizontal (oxygen threshold) or vertical (nitrogen threshold) line. In order to pick best low and high thresholds, parameters of the decision making tree were varied and Receiver Operating Characteristics (ROC) curves were plotted. In signal detection theory, a ROC curve is a graphical plot of true positive rate (or sensitivity) versus false positive rate for a binary classifier system as its discrimination threshold is varied. The ROC-analysis provides tools to select possibly optimal decision boundaries. The ROC curve methodologies are discussed elsewhere (Fawcett, 2006).
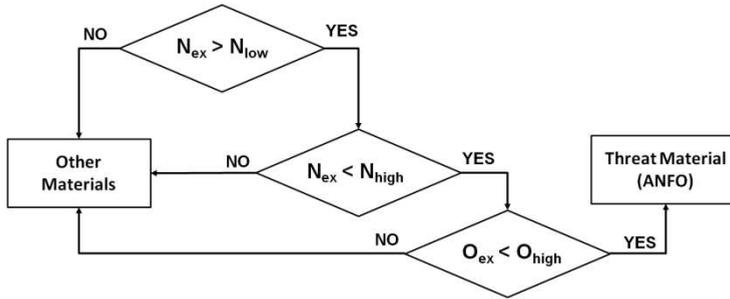
Fig. 8. Example of the decision tree used to analyze data from Fig. 7

Each set of parameters of the decision-making algorithm corresponds to the point on the ROC curve (or ROC surface). Therefore, we define the optimal parameters for the decision-making algorithm as a set of parameters, which allow the minimum "decision" vector magnitude from (0,1) point (left-upper corner of the ROC graph) to the corresponding point on the ROC curve (see Fig.9). The best low and high thresholds were selected by variation of parameters of the decision making tree aimed to determine the ROC curve with the minimal decision vector length. The optimal decision boundaries for identifying the ANFO material are shown as black lines in Fig.7.
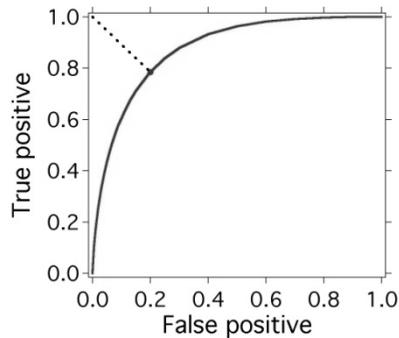
Fig. 9. ROC curve

It is clear that this algorithm does not satisfactory identify substances when classes are overlapping. For example, True Positive rate of the classification between ANFO and urea is only 75%, which is unacceptable for the field deployable system. To improve performance of the classifier, the linear boundary was used. In the case of general linear boundary, the decision making algorithm can be described as the following: if point with experimentally measured nitrogen and oxygen counts (N_{ex}, O_{ex}) lies below the line that is defined as $O = k \cdot N + \ell$, then this point belongs to the class A, if it lies above that line, then it belongs to the class B. The parameters for the linear boundary (the slope and the offset) were varied, and the ROC curves were generated. The optimal pair of parameters corresponds to the minimal decision vector magnitude. This approach tested with the same data set as shown in Fig. 7 produced better results: true positive rates for all classifiers are better than 95%. Optimal linear boundaries are shown in Fig.10 as black lines.
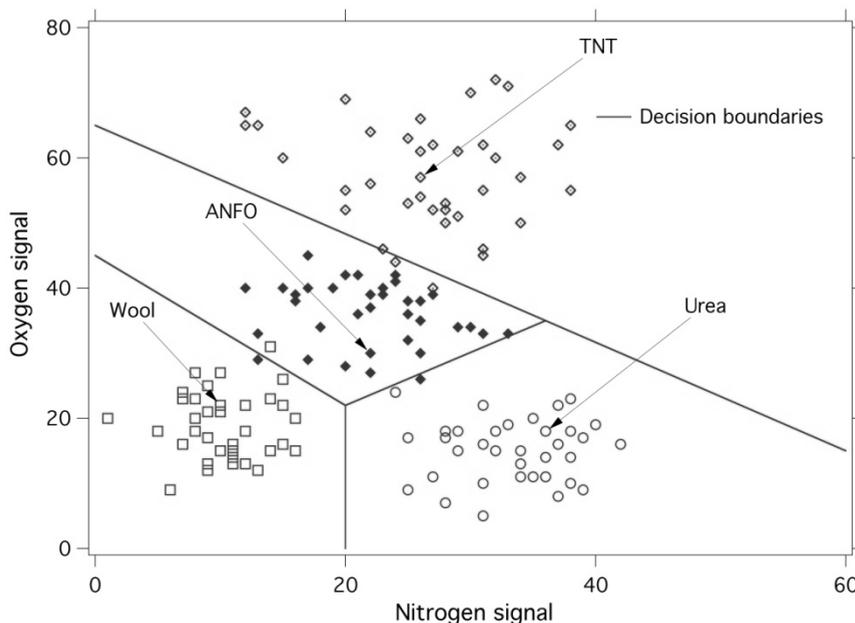
Fig. 10. Linear boundaries between four classes

The use of linear boundaries is significantly improving the material identification capabilities of the neutron based system. The use of polynomial functions is a natural generalization of this approach. Other pattern recognition methods can also be used to construct the decision boundaries of complex shapes and can be applied to analyze the detector signals - for example, methods based on R-functions (Bougaev & Urmanov, 2005).

7. Conclusion

This chapter provided an overview of several material analysis methods using different nuclear reactions induced by pulse neutrons: PGNAA, PFNA, PFTNA, PFTNS, and API. These methods utilize the characteristic gamma radiation and other radiation signatures, prompt and delayed in time, to measure the elemental content of unknown bulk samples. The pulse neutron based elemental analysis is the non-intrusive, non-destructive technique that has yielded the development of in situ material characterization systems in many areas: process control in industry, medicine, security, geological and environmental studies, and others. These applications require automatic, rapid spectra analysis and sample classification algorithms to be effective for the real world use. The methods of spectral decomposition using the combination of single element's detector responses proved to be effective. The pattern recognition methods shown true positive rates ~95% in the material classification.

8. References

Aleksandrov, V.D.; Bogolubov, E.P.; Bochkarev, O.V.; Korytko, L.A.; Nazarov, V.I.; Polkanov, Yu.G.; Ryzhkov, V.I. & Khasaev, T.O. (2005). Application of Neutron

Generators for High Explosives, Toxic Agents and Fissile Material Detection, *Applied Radiation and Isotopes*, Vol. 63, pp. 537-543, ISSN 0969-8043

April, E.; Bolotnikov, A.E.; Bolozdynya, A.I & Doke, T. (2006). *Noble Gas Detectors*, Wiley-VCH, 1st Edition, ISBN 978-3527405978

Barzilov, A. & Womble, P.C. (2006). Comparison of Gamma-Ray Detectors for Neutron-Based Explosives Detection Systems, *Transactions of American Nuclear Society*, Vol. 94, p. 543, ISSN 0003-018X

Barzilov, A. & Womble, P.C. (2003). NELIS - a Neutron Inspection System for Detection of Illicit Drugs, *AIP Conference Proceedings,* Vol. 680, pp. 939-942, ISSN 1551-7616

Bougaev, A. & Urmanov, A. (2005). R-functions Based Classification for Abnormal Software Process Detection, In: *Computational Intelligence and Security*, J. Carbonell and J. Siekmann, (Eds.), 991-996, Lecture Notes in Computer Science, Vol. 3801/2005, Springer, ISBN 3-540-30818-0, Berlin / Heidelberg, Germany

Chunmei, Z. (2001). Thermal-Neutron Capture Data Update and Revision for Some Nuclides with A>190, INDC-CPR-0055, Nuclear Data Services, International Atomic Energy Agency, Vienna, Austria

Chunmei, Z. (2000). Thermal Neutron Capture Data for A=1-25, INDC-CPR-0051, Nuclear Data Services, International Atomic Energy Agency, Vienna, Austria

Cooper, J.C.; Koltick, D.S.; Mihalczo, J.T. & Neal, J.S. (2003). Evaluation of ZnO(Ga) Coatings as Alpha Particle Transducers within a Neutron Generator, *Nuclear Instruments and Methods in Physics Research A*, Vol. 505, Issues 1-2, pp. 498-501, ISSN 0168-9002

Cooper, J.C. & Koltick, D.S. (2001). Optimization of Time and Energy Resolution at High Count Rates with a Large Volume Coaxial High Purity Germanium Detector, *Nuclear Science Symposium Conference Record*, IEEE, Vol.4, pp. 2420-2423, ISBN 0-7803-7324-3

Demidov, A.M.; Govor, L.I. & Cherepantsev, Yu.K. (1978). *Atlas of Gamma-Ray Spectra from Inelastic Scattering of Reactor Fast Neutrons*, INDC-CCP-120, Nuclear Data Services, International Atomic Energy Agency, Vienna, Austria

Dep, L.; Belbot, M.; Vourvopoulos, G. & Sudar, S. (1998). Pulsed Neutron-Based On-Line Coal Analysis, *Journal of Radioanalytical and Nuclear Chemistry*, Vol. 234, No.1-2, pp. 107-112, ISSN 0236-5731

Eleon, C.; Perot, B.; Carasco, C.; Sudac, D.; Obhodas, J. & Valcovic, V. (2010). Experimental and MCNP Simulated Gamma-Ray Spectra for the UNCOSS Neutron-Based Explosive Detector, *Nuclear Instruments and Methods in Physics Research A*, Vol. 629, pp. 220-229, ISSN 0168-9002

Fawcett, T. (2006). An introduction to ROC analysis, *Pattern Recognition Letters*, Vol. 27, pp. 861–874, ISSN 0167-8655

Fourches, N.; Walter, G. & Bourgoin, J.C. (1991). Neutron-Induced Defects in High-Purity Germanium, *Journal of Applied Physics*, Vol. 69, pp. 2033-2043, ISSN 0021-8979

Gozani, T. (1995). Understanding the Physics Limitations of PFNA - the Nanosecond Pulsed Fast Neutron Analysis, *Nuclear Instruments and Methods in Physics Research B*, Vol. 99, pp. 743-747, ISSN 0168-583X

Holslin, D.T.; Shyu, C.M.; Sullivan, R.A. & Vourvopoulos, G. (2006). PELAN for Non-Intrusive Inspection of Ordnance, Containers, and Vehicles, *Proceedings of SPIE*, Vol. 6213, p. 621307, ISSN 0277-786X

James, W.D. & Fuerst, C.D. (2000). Overcoming Matrix Effects in the 14-MeV Fast Neutron Activation Analysis of Metals, *Journal of Radioanalytical and Nuclear Chemistry*, Vol. 244, No.2, pp. 429-434, ISSN 0236-5731

Kessler, B. (2010). An Algorithm for Wavelet–Based Elemental Spectrum Analysis, 13th International Conference on Approximation Theory, San Antonio, TX, March 7-10, 2010. Available at: http://works.bepress.com/bruce_kessler/65

Koltick, D.S.; Kane, S.Z.; Lvovsky, M.; Mace, E.K.; McConchie, S.M. & Mihalczo, J.T. (2009). Characterization of an Associated Particle Neutron Generator With ZnO:Ga Alpha-Detector and Active Focusing, *IEEE Transactions on Nuclear Science*, Vol. 56, pp. 1301-1305, ISSN 0018-9499

Koltick, D.S; Kim, Y.; McConchie, S.; Novikov, I.; Belbot, M. & Gardner, G. (2007). A Neutron Based Vehicle-Borne Improvised Explosive Device Detection System, *Nuclear Instruments and Methods in Physics Research B*, Vol. 261, pp. 277-280, ISSN 0168-583X

Lanza, R. (2007). Nuclear Techniques for Explosive Detection: Current Prospects and Requirements for Future Development, In: *Combined Devices for Humanitarian Demining and Explosive Detection*, International Atomic Energy Agency, ISBN 978-92-0-157007-9, Vienna, Austria

Ljungvall, J. & Nyberg, J. (2005). A Study of Fast Neutron Interactions in High-Purity Germanium Detectors, *Nuclear Instruments and Methods in Physics Research A*, Vol. 546, pp. 553–573, ISSN 0168-9002

Lone, M.A.; Leavitt, R.A. & Harrison, D.A. (1981). Prompt Gamma Rays from Thermal-Neutron Capture, *Atomic Data and Nuclear Data Tables*, Vol. 26, Issue 6, pp. 511-559, ISSN 0092-640X

Maglich, B.C. & Nalcioglu, O. (2010). ONCOSENSOR for Noninvasive High-Specificity Breast Cancer Diagnosis by Carbogen-Enhanced Neutron Femto-Oximetry, *ASME Conference Proceedings: Congress on NanoEngineering for Medicine and Biology*, pp. 57-58, ISBN 978-0-7918-4392-5

Nikitin, A. & Bliven, S. (2010). Needs of Well Logging Industry in New Nuclear Detectors, *Nuclear Science Symposium Proceedings*, pp. 1214-1219, Knoxville, TN, Oct. 30 – Nov. 6, 2010, ISSN 1082-3654

NNMAB-482-6 (1999). *The Practicality of Pulsed Fast Neutron Transmission Spectroscopy for Aviation Security*, National Academies Press, ISBN 0-309-07367-7

Overley, J.C.; Chmelik, M.S.; Rasmussen, R.J.; Schofield, R.M.S.; Sieger, G.E. & Lefevre, H.W. (2006). Explosives Detection via Fast Neutron Transmission Spectroscopy, *Nuclear Instruments and Methods in Physics Research Section B*, Vol. 251, pp. 470-478, ISSN 0168-583X

Parsons, A.; Bodnarik, J.; Evans, L.; Floyd, S.; Lim, L.; McClanahan, T.; Namkung, M.; Nowicki, S.; Schweitzer, J.; Starr, R. & Trombka, J. (2011). Active Neutron and Gamma-Ray Instrumentation for In-Situ Planetary Science Applications, *Nuclear Instruments and Methods in Physics Research A*, Vol. 652, pp. 674-679, ISSN 0168-9002

Pehl, R.H.; Madden, N.W.; Elliott, J.H.; Raudorf, T.W.; Trammel, R.C & Darken, L.S. (1979). Radiation Damage Resistance of Reverse Electrode Ge Coaxial Detectors, *IEEE Transactions on Nuclear Science*, Vol. 26, pp. 321-323, ISSN 0018-9499

Perret, G.; Perot, B.; Artaud, J-L. & Mariani, A. (2006). EURITRACK Tagged Neutron Inspection System, *Journal of Physics: Conference Series*, Vol. 41, pp. 375-383, ISSN 1742-6596

Reber, E.L.; Blackwood, L.G.; Edwards, A.J.; Jewell, J.K.; Rohde, K.W.; Seabury, E.H. & Klinger, J.B. (2005). Idaho Explosives Detection System, *Nuclear Instruments and Methods in Physics Research B*, Vol. 241, Issue 1-4, pp. 738-742, ISSN 0168-583X

Sangsingkeow, P.; Berry, K.D.; Dumas, E.J.; Raudorf, T.W. & Underwood, T.A. (2003). Advances in Germanium Detector Technology, *Nuclear Instruments and Methods in Physics Research A*, Vol. 505, pp. 183-186, ISSN 0168-9002

Shypailo, R.J. & Ellis, K.J. (2005). Design Considerations for a Neutron Generator-Based Total-Body Irradiator, *Journal of Radioanalytical and Nuclear Chemistry*, Vol. 263, No. 3, pp. 759-765, ISSN 0236-5731

Shyu, C. M.; Gardner, R.P. & Verghese, K. (1993). Development of the Monte Carlo Library Least-Squares Method of Analysis for Neutron Capture Prompt Gamma-Ray Analyzers, *Nuclear Geophysics*, Vol. 7, No. 2, pp. 241-268, ISSN 0969-8086

Sowerby, B.D. (2009). Nuclear techniques for the On-Line Bulk Analysis of Carbon in Cola-Fired Power Stations, *Applied Radiation and Isotopes*, Vol. 67, pp. 1638-1643, ISSN 0969-8043

Strellis, D. A.; Gozani, T. & Stevenson, J. (2009). Air Cargo Inspection Using Pulsed Fast Neutron Analysis**,** In: *IAEA Proceedings Series: Topical Meeting on Nuclear Research - Applications and Utilization of Accelerators*, Paper SM/EN-05, International Atomic Energy Agency, ISBN 978-92-0-150410-4, Vienna, Austria

Tsoulfanidis, N. & Landsberger, S. (2010). *Measurement and Detection of Radiation*, 3rd Edition, CRC Press, ISBN 1420091859

Vakhtin, D.N.; Gorshkov, I.Yu.; Evsenin, A.V.; Kuznetsov, A.V. & Osetrov, O.I. (2006). Senna – Portable Sensor for Explosives Detection Based on Nanosecond Neutron Analysis, In: *Detection and Disposal of Improvised Explosives*, H. Schubert and A. Kuznetsov, (Eds.), 87-96, NATO Security through Science Series B: Physics and Biophysics, Vol. 6, Springer, ISBN 1-4020-4886-6, Dordrecht, The Netherlands

van Loef, E.V.D. , Dorenbos, P; van Eijk, C.W.E; Gudel, H.U. & Kraemer, K.W. (2001). High-Energy-Resolution Scintillator: Ce^{3+} activated $LaBr_3$, *Applied Physics Letters*, Vol. 79, No. 10, pp. 1573-1575, ISSN 0003-6951

Vourvopoulos, G. & Womble, P. (2001). Pulsed Fast Thermal Neutron Analysis: A Technique for Explosives Detection, *Talanta*, Vol. 54, pp. 459-468, ISSN 0039-9140

Wielopolski, L.; Hendrey, G.; Johnsen, K.; Mitra, S.; Prior, S.; Rogers, H. & Tolbert, H. (2008). Nondestructive System for Analyzing Carbon in the Soil, *Soil Science Society of America Journal*, Vol. 72, pp. 1269-1277, ISSN 0361-5995

Williams, D. L.; Vainionpaa, J. H.; Jones, G.; Piestrup, M. A.; Gary, C. K.; Harris, J. L.; Fuller, M. J.; Cremer, J. T.; Ludewigt, B. A.; Kwan, J. W.; Reijonen, J.; Leung, K.-N. & Gough, R. A. (2008). High Intensity, Pulsed, D-D Neutron Generator, *AIP Conference Proceedings*, Vol. 1099, pp. 936-939, ISSN 1551-7616

Womble, P.C.; Barzilov, A.; Novikov, I.; Howard, J. & Musser, J. (2009). Evaluation of the Doppler-Broadening of Gamma-Ray Spectra from Neutron Inelastic Scattering on Light Nuclei, *AIP Conference Proceedings*, Vol. 1099, pp. 624-627, ISSN 1551-7616

Womble, P.C.; Paschal, J. & Moore, R. (2005). Cement Analysis Using d + D neutrons, *Nuclear Instruments and Methods in Physics Research B*, Vol. 241, No.1-4, pp. 765-769, ISSN 0168-583X

Womble, P.C.; Vourvopoulos, G.; Paschal, J.; Novikov, I. & Chen, G. (2003). Optimizing the Signal-to-Noise Ratio for the PELAN System, *Nuclear Instruments and Methods in Physics Research A*, Vol. 505, Issue 1-2, pp. 470-473, ISSN 0168-9002

Womble, P.C.; Vourvopoulos, G.; Paschal, J.; Novikov, I. & Barzilov, A. (2002). Results of Field Trials for the PELAN System, *Proceedings of SPIE*, Vol. 4786, pp. 52-57, ISSN 0277-786X

Womble, P.C.; Schultz, F.J. & Vourvopoulos, G. (1995). Non-Destructive Characterization Using Pulsed Fast-Thermal Neutrons, *Nuclear Instruments and Methods in Physics Research B*, Vol. 99, pp. 757-760, ISSN 0168-583X
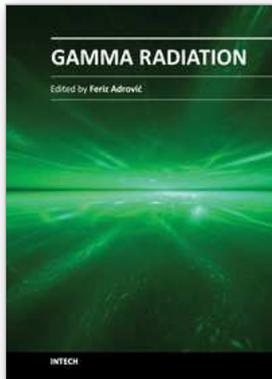
Gamma Radiation

Edited by Prof. Feriz Adrovic

This book brings new research insights on the properties and behavior of gamma radiation, studies from a wide range of options of gamma radiation applications in Nuclear Physics, industrial processes, Environmental Science, Radiation Biology, Radiation Chemistry, Agriculture and Forestry, sterilization, food industry, as well as the review of both advantages and problems that are present in these applications. The book is primarily intended for scientific workers who have contacts with gamma radiation, such as staff working in nuclear power plants, manufacturing industries and civil engineers, medical equipment manufacturers, oncologists, radiation therapists, dental professionals, universities and the military, as well as those who intend to enter the world of applications and problems of gamma radiation. Because of the global importance of gamma radiation, the content of this book will be interesting for the wider audience as well.

How to reference

In order to correctly reference this scholarly work, feel free to copy and paste the following:

Alexander P. Barzilov, Ivan S. Novikov and Phillip C. Womble (2012). Material Analysis Using Characteristic Gamma Rays Induced by Neutrons, Gamma Radiation, Prof. Feriz Adrovic (Ed.), ISBN: 978-953-51-0316-5, InTech, Available from: http://www.intechopen.com/books/gamma-radiation/material-analysis-using-characteristic-gamma-rays-induced-by-pulse-neutrons

INTECH
open science | open minds